Filter Banks for Time-Recursive Implementation of Transforms

Mukund Padmanabhan, *Member, IEEE,* and Ken Martin, *Fellow, IEEE*

***Abstract*—A generalized filter-bank structure is developed, to implement an arbitrary transform in a time-recursive manner. It is based on the NxN basis matrix of the transform, and for the general case, has a complexity of $O(N^2)$; however, its complexity reduces considerably, to approximately $4N - 5N$, for the case of trigonometric transforms such as the DFT, DCT, and DST. As far as hardware complexity is concerned, it is similar to frequency sampling structures, but unlike them, it has much better behavior under finite precision arithmetic; it remains stable under coefficient truncation, and also does not sustain limit cycles if magnitude truncation is applied. The linear complexity, modularity, and good finite precision behavior of the structure make it extremely suitable for implementation using VLSI circuits or digital signal processors.**

I. Introduction

THE NEED to apply a transformation on a data vector is one that arises in several applications such as frequency domain adaptive filtering [1], [2], data compression [3], etc. Consequently, a great deal of attention has been devoted to the development of efficient structures to implement these transforms. As most of the commonly used transforms have basis matrices that are related to trigonometric functions, most methods take advantage of their periodicity to obtain order-recursive schemes to efficiently compute the transform. The usual drawback of these approaches is the extensive data reordering that is needed to implement them, which makes a VLSI implementation of the transformer very difficult. In contrast, time-recursive solutions [1], [4]-[6], [7, ch. 6] result in very simple and modular digital filter structures, that do not need any data reordering, and at the same time have a low hardware complexity (the time-recursive structure is, however, required to operate at the same rate as the incoming data). Most of the time-recursive schemes advocate the use of a frequency-sampling structure. Unfortunately, however, the frequency-sampling structure has poor behavior under finite precision because it relies on a pole-zero cancellation on the unit circle; consequently, slight mismatches may result in the structure having a pole on, or very close to the unit circle.

This problem may be solved for the case of the DFT by using the nice alternative to the frequency sampling structure proposed in [6]; unfortunately, however, the method of [6] cannot be extended to the case of the more commonly used transforms such as the DCT or DST. In this paper, we show how to implement the time recursive transformer for any trigonometric transform, using structures similar to the one in [6]. The formulation of this time-recursive solution is motivated by the earlier work of [6], [8], [9]; however, unlike the earlier approaches which were based on observer theory, the underlying theory is developed in a different way, that is simpler and based entirely in the z-domain. It is also more general, and may be applied to any transform; further, the filters of [6], [9] can be arrived at using this generalized approach. For the completely general case, the structure does not yield any computational saving, having a complexity of $O(N^2)$; however, for the case of trigonometric transforms, its complexity reduces greatly, to the same level as that of an equivalent frequency sampling structure; i.e., $O(N)$. Unlike the frequency sampling structure, however, it has much better sensitivity properties. In particular, the structure remains stable under finite coefficient precision, does not sustain zero input limit cycles, and also has low roundoff noise.

This paper is organized as follows. A general filter structure to implement arbitrary transforms in a time-recursive manner is developed first. For the completely general case, the resulting structure is not very useful; however, it provides a framework for the development of very efficient and "good" structures for the case of trigonometric transforms. Subsequently, the structure is specialized to the case of trigonometric transforms (such as the DCT, DST, DFT), and compared with some other techniques to compute sliding transforms [1], [5]. Finally, the effects of finite precision on the filter structure are examined.

The following notations will be used in the paper: underlined lowercase letters will represent vectors, underlined uppercase letters will represent matrices, $*$ will denote transposition of the complex conjugate, and the operation $\lfloor x \rfloor$ will be used to denote the greatest integer less than or equal to x.

II. Recursive Filter Structures To Implement Transforms

Consider a transform with the basis matrix

$$\underline{H} = \begin{bmatrix} h_{0,0} & \cdots & h_{0,N-1} \\ \vdots & \ddots & \vdots \\ h_{N-1,0} & \cdots & h_{N-1,N-1} \end{bmatrix}. \tag{1}$$

A "sliding" transform of the input data may be obtained by passing the data through a bank of N FIR filters, with the

Manuscript received August 8, 1990; revised April 15, 1991, March 10, 1992, October 26, 1992, and November 10, 1992. This work was supported in part by the National Science Foundation under Grant MIP-8913164. This paper was recommended by Associate Editor D.C. Farden.

M. Padmanabhan is with the IBM T.J. Watson Research Center, Yorktown Heights, NY 10598.

K. Martin is with the Electrical Engineering Department, University of Toronto, Toronto, Canada M5S 1A4.

IEEE Log Number 9207965.

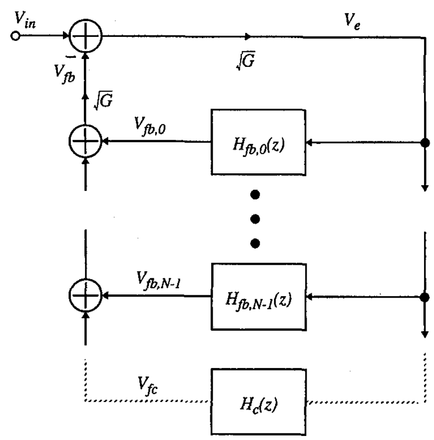

Fig. 1. Generalized filtering structure.

transfer function of the ith filter being related to the elements of the ith row of the basis matrix [10], [11], i.e.,

$$H_{bp,i}(z) = h_{i,N-1}z^{-1} + \cdots + h_{i,0}z^{-N}. \qquad (2)$$

The generalized structure described in this paper implements this transfer function using a feedback loop, which results in improved sensitivity properties as shown later. The structure contains certain "basis generating" IIR filters, and a "compensating" filter, in a feedback loop, and its capability to perform transformations is dependent on choosing the "compensating" filter coefficients in such a way that the overall structure resembles an FIR filter, with all its poles at 0.[1] The term "basis-generating" is used because the filters can be considered as a cascade of an IIR filter, $\frac{1}{1 \pm z^{-K}}$ (K is an integer that is dependent on the transform to be implemented), and an FIR filter $H_{bp,i}(z)$; the IIR filter can be thought of as producing an impulse every K sample periods, that excites the FIR filter, and the impulse response of the filter is hence a periodic sequence related to the ith row of the basis matrix.

The overall filter structure is shown in Fig. 1, with the filter $H_{fb,i}(z)$ representing the ith "basis-generating" filter, and $V_{fb,i}$ being the ith output of the filter-bank. The transfer functions of $H_{fb,i}(z)$ and $H_c(z)$ are given by

$$H_{fb,i}(z) = \frac{V_{fb,i}}{V_e} = \frac{H_{bp,i}(z)}{1+\eta z^{-K}} \quad i = 0, \cdots, N-1 \qquad (3)$$

$$H_c(z) = \frac{V_{fc}}{V_e} = \frac{[h_{c,1}z^{-1} + \cdots + h_{c,N}z^{-N}]}{1+\eta z^{-K}} \quad \text{for } K \le N \qquad (4)$$

$$\text{or } H_c(z) = \frac{[h_{c,1}z^{-1} + \cdots + h_{c,K-1}z^{-(K-1)}]}{1+\eta z^{-K}} \quad \text{for } K > N \qquad (5)$$

[1] This is seen to be related to the imposition of 'deadbeat' behavior on the identity observer of [6], [8], [9], [12]. The error between the states of the hypothetical system, and the identity observer, that is attempting to reconstruct its states, goes to zero in N samples in a "deadbeat" observer. This is done by appropriately setting the observer gain vector.

where $\eta = \pm 1$. The following derivations assume that $K \le N$; they may be easily extended to the case where $K > N$. The loop gain of the structure shown in Fig. 1 is given by

$$\begin{aligned} \delta(z) &= G\left[H_c(z) + \sum_{i=0}^{N-1} H_{fb,i}(z)\right] \\ &= \frac{G}{1+\eta z^{-K}} \sum_{j=1}^{N}\left[h_{c,j} + \sum_{i=0}^{N-1} h_{i,N-j}\right] z^{-j}. \end{aligned} \qquad (6)$$

If we choose the coefficients $h_{c,j}$ and $\sqrt{G}$ such that the following conditions are satisfied,

$$\left\{\begin{array}{ll} h_{c,j} = -\sum_{i=0}^{N-1} h_{i,N-j} & j = 1, \cdots, N \quad j \ne K \\ h_{c,K} = 0 & \\ G = \frac{-\eta}{\sum_{i=0}^{N-1} h_{i,N-K}} & \end{array}\right\}, \qquad (7)$$

then the loop gain becomes

$$\delta(z) = \frac{-\eta z^{-K}}{1+\eta z^{-K}} \qquad (8)$$

and we obtain the transfer function from the input to the error, V_e, and to the fedback signal, V_{fb}, as

$$\begin{aligned} H_e(z) &= \frac{V_e}{V_{in}} = \frac{\sqrt{G}}{1+\delta(z)} = \sqrt{G}(1+\eta z^{-K}) \\ \text{and } H_{fb}(z) &= \frac{V_{fb}}{V_{in}} = \frac{\delta(z)}{1+\delta(z)} = -\eta z^{-K}. \end{aligned} \qquad (9)$$

Hence, the overall filter behaves like an FIR filter.[2] If the basis matrix H is such that all column sums, except the $(N-K)$th, are equal to zero, then from (7), $h_{c,j} = 0$, and no compensating filter is required. This condition holds true for the basis matrices of transforms such as the DFT and the WHT for $K = N$; however, for some special cases such as the DCT and DST, even though these conditions do not hold true, we do not need to include a separate compensating filter in the feedback loop, as is shown later.

2.1. Sequence-to-Vector Transformation

If the input data is available sequentially in time, and if $h_{c,j}$ and $\sqrt{G}$ are chosen as in (7), from (3) and (9), $V_{fb,i}(z) = H_{fb,i}(z)H_e(z)V_{in}(z) = \sqrt{G}H_{bp,i}(z)V_{in}(z)$; i.e., the transfer function from the input to the ith filter-bank output, scaled by $1/\sqrt{G}$, gives $H_{bp,i}(z)$. The desired transformation can now be obtained by scaling the $V_{fb,i}$ outputs by $1/\sqrt{G}$, which due to the finite memory of the overall filter, will yield the transform of the last N data samples at any instant. As the input to the transformer is a sequence and the output is a vector, it will be referred to in the subsequent text as a sequence to vector $(S-V)$ structure.

[2] If the $H_{fb,i}(z)$ are implemented using N delays, then it is always possible to choose the $h_{c,j}$ such that the first two conditions of (7) are satisfied. Further, if finite precision constrains the actually implemented value of $\sqrt{G}$ to be equal to $\gamma\sqrt{G}$, where $\gamma \le 1$, then the transfer function $H_e(z)$ may be obtained as $H_e(z) = \gamma\sqrt{G}(1+\eta z^{-K})/(1+\eta(1-\gamma^2)z^{-K})$. The poles of the filter structure may now be seen to be evenly distributed around the unit circle at a radius of $(1-\gamma^2)^{1/K}$ (for infinite precision, $\gamma = 1$, and the poles are all at 0). Hence, the filter remains stable even if finite precision is used to represent $\sqrt{G}$.

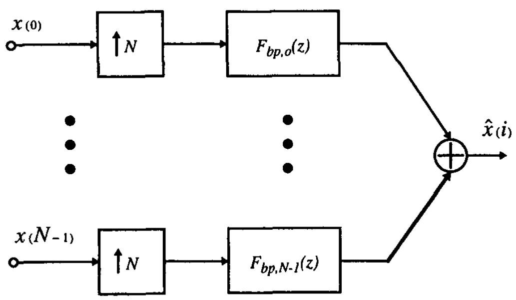

Fig. 2. "Vector-to-sequence" structure.

2.2. Vector-to-Sequence Transformation

In some situations (e.g., synthesis-banks for multirate systems), the data to be transformed may be available in the form of an Nx1 vector $\underline{x}$ at time $t=0$, and it may be desired to compute the transformation $\underline{H}^T\underline{x}$. This may be done by the system shown in Fig. 2[3] if

$$F_{bp,i}(z) = z^{-(N+1)} H_{bp,i}(z^{-1}), \tag{10}$$

with $H_{bp,i}(z)$ as given in (2). This can be easily seen because the output at the ith time instant, $\hat{x}(i)$, is the inner product of the vector $\underline{x}$ and the ith column of $\underline{H}$, so the elements of the desired vector, $\hat{\underline{x}} = \underline{H}^T\underline{x}$, are available as a sequence of samples in time. Hence, the filter-bank of Fig. 2 implements a "Vector-to-Sequence" transformation, and will be referred to as the V-S structure in the following text. The N-input single-output V-S structure can be implemented by first designing an S-V structure, with its basis generating filters redefined as $H_{fb,i}(z) = F_{bp,i}(z)/(1+\eta z^{-K})$, and with the coefficients of the compensating filter chosen as

$$\left\{\begin{array}{ll} h_{c,j} = -\sum_{i=0}^{N-1} h_{i,j-1} & j=1,\cdots,N \quad j\neq K \\ h_{c,K} = 0 & \\ G = \frac{-\eta}{\sum_{i=0}^{N-1} h_{i,K-1}} & \end{array}\right\}. \tag{11}$$

Subsequently the V-S structure may be implemented as the *transpose* of the above structure.

III. Implementation Of Different Transforms

Both the S-V and V-S structures, in their general form, require N^2 multiplications. For the specific case of the DCT, DST, DFT, and the corresponding inverse transforms, however, the structures simplify considerably, and ultimately require only $4N$ to $6N$ multiplications (see Table V). The structures based on the DFT and WHT reported in [6] and [9] will be shown here to arise as special cases of the S-V structure, and, in addition, the implementation of the various forms of the DCT and the DST will also be considered.

3.1. S-V Structures

We will first consider the implementation of the DFT and a related transform, as these will provide the building blocks to implement the other transforms.

[3]The function of the interpolators is to interpolate $N-1$ zeros between successive received data samples.

TABLE I
DFT-Based Filter-Bank

DFT	$\eta=-1$, $K=N$	$H_{fb,i}(z) = \frac{-\eta z_i^* z^{-1}}{1-z_i^* z^{-1}}$	$z_i = w_N^i$, $w_N = e^{j\frac{2\pi}{N}}$ $i=0,\cdots,N-1$
		$h_{c,j}=0$	$j=1,\cdots,N-1$
		$\sqrt{G} = \frac{-\eta}{\sqrt{N}}$	

3.1.1. DFT: The (l,m)th element of the DFT basis matrix is given by w_N^{lm} $(l,m=0,\ldots,N-1)$, where $w_N = e^{j\frac{2\pi}{N}}$. From (2) and (3),

$$H_{fb,i}(z) = \frac{1-z^{-N}}{1+\eta z^{-K}} \frac{z_i^* z^{-1}}{1-z_i^* z^{-1}}, \tag{12}$$
$$\text{where } z_i = w_N^i, \text{ and } i=0,\ldots,N-1.$$

Now, if we choose $\eta=-1$, and $K=N$, the expression for the $H_{fb,i}(z)$ becomes $-\eta z_i^* z^{-1}/(1-z_i^* z^{-1})$, and this may be implemented with a single delay, and the overall structure with a canonical number (N) of delays. This turns out to be a necessary condition for the low sensitivity of the structure (see Appendix A.1). Further, all column sums of the DFT matrix, except the first, are seen to sum to zero; hence, no compensating filter is needed and we only need to choose $\sqrt{G} = \frac{-\eta}{\sqrt{N}}$, to obtain FIR behavior. These conditions are summarized in Table I, and it is seen that the filter structure reduces to the one proposed in [9].

We will next consider a related structure that will be useful in the following sections. A related basis matrix may be defined, whose elements are given by $\left\{w_{2N}^{(2l+1)m}\right\}$. The filter-bank associated with this basis matrix takes exactly the same form as the DFT based structure (see Table I), with the difference that $\eta=1$, and the z_i are now given by w_{2N}^{2i+1}.

Both the DFT-based and related structure are seen to take the form of real and complex first-order resonators in a feedback loop, with the resonator frequencies being the N roots of $-\eta$.[4] In order to implement these structures using real multipliers, a pair of first order resonators with complex conjugate poles may be grouped together to yield a biquad with real coefficients; i.e.,

$$\begin{aligned} H_{fb,ii^*}(z) &= \frac{z_i z^{-1}}{1-z_i z^{-1}} + \frac{z_i^* z^{-1}}{1-z_i^* z^{-1}} \\ &= \frac{2\cos(\theta_i)z^{-1} - 2z^{-2}}{1-2\cos(\theta_i)z^{-1}+z^{-2}}, \end{aligned} \tag{13}$$

where

$$\begin{bmatrix} \theta_i = \frac{2\pi i}{N},\ i=1,\ldots,\lfloor\frac{N-1}{2}\rfloor & \text{for the DFT case} \\ \theta_i = \frac{\pi(2i-1)}{N},\ i=1,\ldots,\lfloor\frac{N}{2}\rfloor+1 & \text{for the modified DFT case} \end{bmatrix}. \tag{14}$$

The DFT or modified-DFT-based structure embeds these $H_{fb,ii^*}(z)$ in a feedback loop. In addition (depending on whether N is even or odd), it may also embed real first order resonators, with the transfer functions $z^{-1}/1-z^{-1}$ or $-z^{-1}/1+z^{-1}$, in the feedback loop.

[4]It was pointed out in [13] that if the filter structure is to be orthogonal, and FIR, the only possible sets of resonator frequencies are the N roots of 1 or -1.

3.1.2. Walsh Hadamard Transform: To implement the WHT, if we choose $K = N$ and $\eta = -1$, we see that we do not need a compensating filter. Further, expressing $H_{fb,i}(z)$ as the sum of N partial fractions having the N roots of unity as their roots, we arrive at the structure of [9].

3.1.3. General Trigonometric Transforms: Under the category of general trigonometric transforms, we group the various forms of the DCT and the DST [5]. The general case here does need a compensating filter in order to impose FIR behavior on the overall structure. However, it turns out to be unnecessary to have a separate compensating filter in the feedback loop, as the compensating output, V_{fc}, can be obtained from the internal nodes of the $H_{fb,i}(z)$ itself.

Consider the DCT basis matrix proposed in [3] (DCT-II of [5]), whose elements are given by

$$\left\{\sqrt{\frac{2}{N}}k_l \cos\left[l(m+\frac{1}{2})\frac{\pi}{N}\right]\right\}$$

$$k_l = 1 \quad l \neq 0, N, \quad k_0 = k_N = \frac{1}{\sqrt{2}} \quad l, m = 0, \ldots, N-1.$$

The $H_{fb,i}(z)$ for this case can be derived to be

$$H_{fb,i}(z) = -\sqrt{\frac{2}{N}}k_i\left[\frac{z^{-1}(1-z^{-1})\cos(\theta_i/2)}{1-2\cos(\theta_i)z^{-1}+z^{-2}}\right]\left[\frac{z^{-N}-e^{j(\pi i)}}{1+\eta z^{-K}}\right] \tag{15}$$

$$\text{where } \theta_i = \frac{\pi i}{N}, \quad i = 0, \ldots, N-1. \tag{16}$$

We would like to implement the feedback part of the system with a minimal number of delays, because as mentioned earlier, this is a necessary condition for the low sensitivity of the structure under finite coefficient wordlength (see Appendix A.1). In order to do this, we need to separate the $H_{fb,i}(z)$ into two groups, depending on whether i is even or odd, and implement each group using a separate filter bank. We will refer to these henceforth as the "even" and "odd" filter-banks, and differentiate between them when necessary by using the superscript "even" or "odd," respectively, in all relevant quantities. The even and odd filter-banks have $\lfloor\frac{N+1}{2}\rfloor$ and $\lfloor\frac{N}{2}\rfloor$ basis generating filters, respectively.

Consider first the even filter-bank. Choosing $K = N$ and $\eta = -1$, we obtain

$$H_{fb,i}^{even}(z) = \sqrt{\frac{2}{N}}k_i\frac{\cos(\theta_i/2)z^{-1}(1-z^{-1})}{1-2\cos(\theta_i)z^{-1}+z^{-2}}$$
$$\theta_i = \frac{2\pi i}{N} \quad i = 0, \ldots, \left\lfloor\frac{N-1}{2}\right\rfloor. \tag{17}$$

The poles of the $H_{fb,i}^{even}(z)$ are seen to lie at the N roots of unity, and the filter-bank is required to be FIR. One way to do this would be to add a compensating filter, $H_c^{even}(z) = (h_{c,1}^{even}z^{-1} + \cdots + h_{c,N}^{even}z^{-N})/1 - z^{-N}$, in the feedback loop, with the coefficients $h_{c,i}^{even}$ being chosen to give FIR behavior. At this stage, we can save ourselves the trouble of having to compute the $h_{c,i}^{even}$ by making two observations. a) The compensating filter, $H_c^{even}(z)$, may be expressed as the sum of partial fractions, $H_{c,i}^{even}(z), i = 0, \ldots, \lfloor N/2\rfloor$, with the poles of $H_{c,i}^{even}, i = 0, \ldots, \lfloor N-1/2\rfloor$, being the same as the poles of $H_{fb,i}^{even}(z)$; i.e., the roots of unity. The even filter-bank can now be thought of as embedding $\lfloor(N+1)/2\rfloor$ transfer functions, $H_{fbc,i}^{even}(z) \triangleq H_{fb,i}^{even}(z) + H_{c,i}^{even}(z)$, $i = 0, \cdots, \lfloor(N-1)/2\rfloor$ (and for N even, one additional transfer function $H_{c,\frac{N}{2}}^{even}(z) = (-z^{-1})/(1+z^{-1})$) in a feedback loop. b) from Section 3.1.1, for the case where the poles of the basis generating filters are at the roots of unity, FIR behavior is obtained if the filters embedded in the feedback loop have the transfer function (13), and if $\sqrt{G} = 1/\sqrt{N}$.

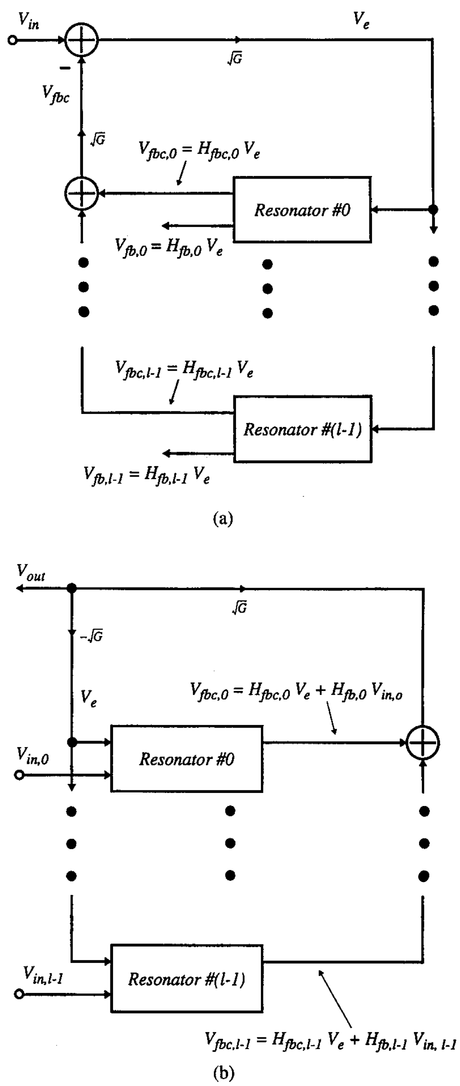

Fig. 3. (a) General form of "even" and "odd" filter-banks of S-V structure. (b) General form of "even" and "odd" filter-banks of V-S structure.

Hence, we may conclude that the transfer functions $H_{fbc,i}^{even}(z)$ are identical to (13), and the even filter-bank, with its compensating filter, has the same feedback structure as the DFT based structure. Likewise, by choosing $K = N$ and $\eta = -1$, a similar connection may be obtained between the odd filter-bank and the modified DFT based structure.

The even and odd filter-banks now take the form shown in Fig. 3(a); *i.e., first- or second-order real resonators in a*

TABLE II
"SEQUENCE-TO-VECTOR" STRUCTURES FOR THE DCT

	$DCT-I$	$\left\{\sqrt{\frac{2}{N}}\, k_i k_j \,\cos\left[\frac{\pi ij}{N}\right]\right\}$	$i,j=0,\cdots,N-1$
Even	$K=N$ $\eta=-1$	$H_{fb,i}^{even}(z)=-\sqrt{\frac{2}{N}}\, k_i\, \frac{z^{-1}(z^{-1}-\cos(\theta_i))}{1-2\cos(\theta_i)z^{-1}+z^{-2}}$ $H_{fbc,i}^{even}(z)$- see (19)	$\theta_i=\frac{2\pi i}{N}\quad i=0,\cdots,\lfloor\frac{N-1}{2}\rfloor$ $\sqrt{G}=\frac{1}{\sqrt{N}}$, $C=\sqrt{\frac{2}{N}}\left(\frac{1}{\sqrt{2}}-1\right)$
Odd	$K=N$ $\eta=1$	$H_{fb,i}^{odd}(z)=\sqrt{\frac{2}{N}}\, \frac{z^{-1}(z^{-1}-\cos(\theta_i))}{1-2\cos(\theta_i)z^{-1}+z^{-2}}$ $H_{fbc,i}^{odd}(z)$- see (19)	$\theta_i=\frac{\pi(2i+1)}{N}\quad i=0,\cdots,\lfloor\frac{N-2}{2}\rfloor$ $\sqrt{G}=\frac{1}{\sqrt{N}}$, $C=\sqrt{\frac{2}{N}}\left(\frac{1}{\sqrt{2}}-1\right)$
	$V_{fb,2i}=V_{fb,i}^{even}+C\,k_i\,V_{fbc}^{even}\quad i=0,\cdots,\lfloor\frac{N-1}{2}\rfloor$ $V_{fb,2i+1}=V_{fb,i}^{odd}-CV_{fbc}^{odd}\quad i=0,\cdots,\lfloor\frac{N-2}{2}\rfloor$		
	$DCT-II$	$\left\{\sqrt{\frac{2}{N}}\, k_i\, \cos\left[i\,(j+0.5)\,\frac{\pi}{N}\right]\right\}$	$i,j=0,\cdots,N-1$
Even	$K=N$ $\eta=-1$	$H_{fb,i}^{even}(z)=\sqrt{\frac{2}{N}}\, k_i\, \frac{\cos(\theta_i/2)z^{-1}(1-z^{-1})}{1-2\cos(\theta_i)z^{-1}+z^{-2}}$ $H_{fbc,i}^{even}(z)$- see (19)	$\theta_i=\frac{2\pi i}{N}\quad i=0,\cdots,\lfloor\frac{N-1}{2}\rfloor$ $\sqrt{G}=\frac{1}{\sqrt{N}}$
Odd	$K=N$ $\eta=1$	$H_{fb,i}^{odd}(z)=-\sqrt{\frac{2}{N}}\, \frac{\cos(\theta_i/2)z^{-1}(1-z^{-1})}{1-2\cos(\theta_i)z^{-1}+z^{-2}}$ $H_{fbc,i}^{odd}(z)$- see (19)	$\theta_i=\frac{\pi(2i+1)}{N}\quad i=0,\cdots,\lfloor\frac{N-2}{2}\rfloor$ $\sqrt{G}=\frac{1}{\sqrt{N}}$
	$V_{fb,2i}=V_{fb,i}^{even}\quad i=0,\cdots,\lfloor\frac{N-1}{2}\rfloor\quad V_{fb,2i+1}=V_{fb,i}^{odd}\quad i=0,\cdots,\lfloor\frac{N-2}{2}\rfloor$		
	$DCT-III$	$\left\{\sqrt{\frac{2}{N}}\, k_j\, \cos\left[(i+0.5)\,j\,\frac{\pi}{N}\right]\right\}$	$i,j=0,\cdots,N-1$
Even	$K=N$ $\eta=j$	$H_{fb,i}^{even}(z)=\sqrt{\frac{2}{N}}\, \frac{jz_iz^{-1}}{1-z_iz^{-1}}$ $H_{fbc,i}^{even}(z)=\frac{z_iz^{-1}}{1-z_iz^{-1}}$	$z_i=e^{j\frac{(2i-0.5)\pi}{N}}\quad i=0,\cdots,N-1$ $\sqrt{G}=\frac{1}{\sqrt{N}}$
Odd	$K=N$ $\eta=-j$	$H_{fb,i}^{odd}(z)=\sqrt{\frac{2}{N}}\, \frac{jz_iz^{-1}}{1-z_iz^{-1}}$ $H_{fbc,i}^{odd}(z)=\frac{z_iz^{-1}}{1-z_iz^{-1}}$	$z_i=e^{j\frac{(2i+0.5)\pi}{N}}\quad j=0,\cdots,N-1$ $\sqrt{G}=\frac{1}{\sqrt{N}}$, $C=\frac{1}{\sqrt{2}}-1$
	$V_{fb,2i}=\frac{1}{2}\left[-V_{fb,N-i}^{even}+V_{fb,i}^{odd}\right]-CV_{fbc}^{odd}\quad i=0,\cdots,\lfloor\frac{N-1}{2}\rfloor$ $V_{fb,2i+1}=\frac{1}{2}\left[-V_{fb,i+1}^{even}+V_{fb,N-i-1}^{odd}\right]-CV_{fbc}^{odd}\quad i=0,\cdots,\lfloor\frac{N-2}{2}\rfloor$		

TABLE III
"SEQUENCE-TO-VECTOR" STRUCTURES FOR THE DCT

	$DST-I$	$\left\{\sqrt{\frac{2}{N}}\,\sin\left[\frac{\pi(i+1)(j+1)}{N}\right]\right\}$	$i,j=0,\cdots,N-2$
Even	$K=N$ $\eta=1$	$H_{fb,i}^{even}(z)=\sqrt{\frac{2}{N}}\, \frac{\sin(\theta_i)z^{-1}}{1-2\cos(\theta_i)z^{-1}+z^{-2}}$ $H_{fbc,i}^{even}(z)$- see (19)	$\theta_i=\frac{\pi(2i+1)}{N}\quad i=0,\cdots,\lfloor\frac{N-2}{2}\rfloor$ $\sqrt{G}=\frac{1}{\sqrt{N}}\quad i=0,\cdots,\lfloor\frac{N-2}{2}\rfloor$
Odd	$K=N$ $\eta=-1$	$H_{fb,i}^{odd}(z)=-\sqrt{\frac{2}{N}}\, \frac{\sin(\theta_i)z^{-1}}{1-2\cos(\theta_i)z^{-1}+z^{-2}}$ $H_{fbc,i}^{odd}(z)$- see (19)	$\theta_i=\frac{2\pi(i+1)}{N}\quad i=0,\cdots,\lfloor\frac{N-3}{2}\rfloor$ $\sqrt{G}=\frac{1}{\sqrt{N}}\quad i=0,\cdots,\lfloor\frac{N-1}{2}\rfloor$
	$V_{fb,2i}=V_{fb,i}^{even}\quad i=0,\cdots,\lfloor\frac{N-2}{2}\rfloor\quad V_{fb,2i+1}=V_{fb,i}^{odd}\quad i=0,\cdots,\lfloor\frac{N-3}{2}\rfloor$		
	$DST-II$	$\left\{\sqrt{\frac{2}{N}}\, k_{i+1}\,\sin\left[\frac{\pi(i+1)(j+0.5)}{N}\right]\right\}$	$i,j=0,\cdots,N-1$
Even	$K=N$ $\eta=1$	$H_{fb,i}^{even}(z)=\sqrt{\frac{2}{N}}\, k_{i+1}\, \frac{\sin(\frac{\theta_i}{2})z^{-1}(1+z^{-1})}{1-2\cos(\theta_i)z^{-1}+z^{-2}}$ $H_{fbc,i}^{even}(z)$- see (19)	$\theta_i=\frac{\pi(2i+1)}{N}\quad i=0,\cdots,\lfloor\frac{N-1}{2}\rfloor$ $\sqrt{G}=\frac{1}{\sqrt{N}}\quad i=0,\cdots,\lfloor\frac{N-2}{2}\rfloor$
Odd	$K=N$ $\eta=-1$	$H_{fb,i}^{odd}(z)=-\sqrt{\frac{2}{N}}\, k_{i+1}\, \frac{\sin(\frac{\theta_i}{2})z^{-1}(1+z^{-1})}{1-2\cos(\theta_i)z^{-1}+z^{-2}}$ $H_{fbc,i}^{odd}(z)$- see (19)	$\theta_i=\frac{2\pi(i+1)}{N}\quad i=0,\cdots,\lfloor\frac{N-2}{2}\rfloor$ $\sqrt{G}=\frac{1}{\sqrt{N}}\quad i=0,\cdots,\lfloor\frac{N-1}{2}\rfloor$
	$V_{fb,2i}=V_{fb,i}^{even}\quad i=0,\cdots,\lfloor\frac{N-1}{2}\rfloor\quad V_{fb,2i+1}=V_{fb,i}^{odd}\quad i=0,\cdots,\lfloor\frac{N-2}{2}\rfloor$		
	$DST-III$	$\left\{\sqrt{\frac{2}{N}}\, k_{j+1}\,\sin\left[\frac{\pi(i+0.5)(j+1)}{N}\right]\right\}$	$i,j=0,\cdots,N-1$
Even	$K=N$ $\eta=j$	$H_{fb,i}^{even}(z)=\sqrt{\frac{1}{2N}}\, \frac{z^{-1}}{1-z_iz^{-1}}$ $H_{fbc,i}^{even}(z)=\frac{z_iz^{-1}}{1-z_iz^{-1}}$	$z_i=e^{j\frac{(2i-0.5)\pi}{N}}\quad i=0,\cdots,N-1$ $\sqrt{G}=\frac{1}{\sqrt{N}}$
Odd	$K=N$ $\eta=-j$	$H_{fb,i}^{odd}(z)=\sqrt{\frac{1}{2N}}\, \frac{z^{-1}}{1-z_iz^{-1}}$ $H_{fbc,i}^{odd}(z)=\frac{z_iz^{-1}}{1-z_iz^{-1}}$	$z_i=e^{j\frac{(2i+0.5)\pi}{N}}\quad i=0,\cdots,N-1$ $\sqrt{G}=\frac{1}{\sqrt{N}}$, $C=\sqrt{\frac{2}{N}}\left(\frac{1}{\sqrt{2}}-1\right)$
	$V_{fb,2i}=V_{fb,N-i}^{even}+V_{fb,i}^{odd}+Cz^{-1}V_{in}\quad i=0,\cdots,\lfloor\frac{N-1}{2}\rfloor$ $V_{fb,2i+1}=-V_{fb,i+1}^{even}-V_{fb,N-i-1}^{odd}+Cz^{-1}V_{in}\quad i=0,\cdots,\lfloor\frac{N-2}{2}\rfloor$		

feedback loop, which represent minimal realizations, with the transfer function from V_e to the ith fedback output, $V_{fbc,i}$, being given by $H_{fbc,i}(z) = H_{fb,ii^*}(z)$ (see(13)), and the transfer function from V_e to the i^{th} output, $V_{fb,i}$, being given by $H_{fb,i}(z)$. Also, the final desired outputs can be obtained by taking linear combinations of the outputs of the two filter-banks, as indicated in Tables II and III.

The same procedure as above can be followed for the other forms of the DCT and DST, and the relevant quantities and transfer functions, together with the definition of the i,jth

TABLE IV
"VECTOR-TO-SEQUENCE" STRUCTURES

	DFT		
	$\eta=-1$ $K=N$	$H^{even}_{fb,i}(z)=\frac{z^{-1}}{1-z_iz^{-1}}$ $H^{even}_{fbc,i}(z)=\frac{z_iz^{-1}}{1-z_iz^{-1}}$	$z_i=e^{j\frac{2\pi i}{N}}\ i=0,\cdots,N-1$ $\sqrt{G}=\frac{1}{\sqrt{N}}$
	$DCT-II$		
Even	$\eta=-1$ $K=N$	$H^{even}_{fb,i}(z)=\sqrt{\frac{2}{N}}\,k_i\,\frac{\cos(\theta_i/2)z^{-1}(1-z^{-1})}{1-2\cos(\theta_i)z^{-1}+z^{-2}}$ $H^{even}_{fbc,i}(z)$- see (19)	$\theta_i=\frac{2\pi i}{N}\ i=0,\cdots,\lfloor\frac{N-1}{2}\rfloor$ $\sqrt{G}=\frac{1}{\sqrt{N}}$
Odd	$\eta=1$ $K=N$	$H^{odd}_{fb,i}(z)=\sqrt{\frac{2}{N}}\,\frac{\cos(\theta_i/2)z^{-1}(1-z^{-1})}{1-2\cos(\theta_i)z^{-1}+z^{-2}}$ $H^{odd}_{fbc,i}(z)$- see (19)	$\theta_i=\frac{\pi(2i+1))}{N}\ i=0,\cdots,\lfloor\frac{N-2}{2}\rfloor$ $\sqrt{G}=\frac{1}{\sqrt{N}}$
	$DST-II$		
Even	$\eta=1$ $K=N$	$H^{even}_{fb,i}(z)=\sqrt{\frac{2}{N}}\,k_{i+1}\,\frac{\sin(\theta_i/2)z^{-1}(1+z^{-1})}{1-2\cos(\theta_i)z^{-1}+z^{-2}}$ $H^{even}_{fbc,i}(z)=$ - see (19)	$\theta_i=\frac{\pi(2i+1)}{N}\ i=0,\cdots,\lfloor\frac{N-2}{2}\rfloor$ $\sqrt{G}=\frac{1}{\sqrt{N}}$
Odd	$\eta=-1$ $K=N$	$H^{odd}_{fb,i}(z)=\sqrt{\frac{2}{N}}\,k_{i+1}\,\frac{\sin(\theta_i/2)z^{-1}(1+z^{-1})}{1-2\cos(\theta_i)z^{-1}+z^{-2}}$ $H^{odd}_{fbc,i}(z)=$ - see (19)	$\theta_i=\frac{2\pi i}{N}\ i=0,\cdots,\lfloor\frac{N-1}{2}\rfloor$ $\sqrt{G}=\frac{1}{\sqrt{N}}$

element of the basis matrix, are summarized in Tables II and III. For the case of the DCT-III, DST-III, DCT-IV, and DST-IV it becomes necessary to use complex filters, and consequently, the implementation is not as computationally efficient as for the other two versions of the DCT and the DST; hence, only the structures corresponding to the DCT I-III and DST I-III are described here. In the following,

$$k_j=1\quad j\neq 0,N,k_0=k_N=\frac{1}{\sqrt{2}} \tag{18}$$

$$H_{fbc,i}(z)=\left\{\begin{array}{ll}\frac{2\cos(\theta_i)z^{-1}-2z^{-2}}{1-2\cos(\theta_i)z^{-1}+z^{-2}} & \theta_i\neq 0,\pi\\ \frac{\cos(\theta_i)z^{-1}-z^{-2}}{1-2\cos(\theta_i)z^{-1}+z^{-2}} & \theta_i=0\text{ or }\pi\end{array}\right\}$$

and

$$\left\{\begin{array}{ll}i=0,\cdots,\lfloor\frac{N-1}{2}\rfloor, & \theta_i=\frac{2\pi i}{N}\text{ if }\eta=-1\\ i=0,\cdots,\lfloor\frac{N-2}{2}\rfloor, & \theta_i=\frac{\pi(2i+1)}{N}\text{ if }\eta=1\end{array}\right\}. \tag{19}$$

3.2. V-S Structure

We will next consider the implementation of the transformation $\underline{H}^T\underline{x}$ using the V-S structure. These structures may be implemented as the transpose of the S-V filter-bank structure, as shown in Fig. 3(b). Here, the transfer function from $V_{in,i}$ to V_{out} is given by $F_{bp,i}(z)$ (10), from $V_{in,i}$ to $V_{fbc,i}$ by $H_{fb,i}(z)=F_{bp,i}(z)/1+\eta z^{-K}$, and from V_e to $V_{fbc,i}$ by $H_{fbc,i}(z)$ $(=H_{fb,i}(z)+H_{c,i}(z))$, where, just as for the S-V structure, we have expressed the compensating filter as the sum of partial fractions $H_{c,i}(z)$, that have the same poles as $H_{fb,i}(z)$. Also, just as for the S-V structure, it is necessary to have an even and odd filter-bank for the DCT and DST case. Table IV gives the relevant transfer functions for $\underline{H}$ equal to the DFT, and some of the DCT and DST basis matrices.

3.3. Comparison with Other Methods

In general, the computation of block transforms arises in applications such as data compression, and several efficient algorithms have been developed to efficiently compute the DCT or DST of a vector [14]–[16]. In terms of number of multiplications and additions, these methods are more computationally efficient than the transformer presented here ([16] needs only 11 multiplications to compute an 8-pt DCT-II); however, the transformer does have the merit of being simple, and requires no data reordering, etc. It also provides a more efficient alternative to compute sliding transforms for applications such as transform domain adaptive filtering [1], [2], [17], as compared to recursive formulas that were developed in [5] (see Table V). Further, it also provides a much more robust alternative to the frequency sampling like structure developed in [1] and [4], because it shows very good behavior under finite precision (no stability problems, etc.), unlike the frequency sampling structure, as shown in the next section. Table V indicates the number of multiplications and additions needed to implement the filter-bank, and this is also equal to the computations necessary to update a "sliding" transform (coupled form biquads (see Fig. 4) are used to

TABLE V
COMPUTATIONAL COMPLEXITY

	Filter Bank		*Recursive Formulae* [5]	
	Mult	*Add*	*Mult*	*Add*
DFT	$(N+2)^*$	$(N+log_2N+1)^*$		
$DCT-I$	k_1+8	$k_1+k_2+k_3+5$	$12N$	$8N$
$DCT-II$	k_1+k_3+3	$k_1+k_2+k_3+5$	$6N$	$6N$
$DCT-III$	$(2N+2)^*+2$	$(4N+2log_2N+2)^*$	$12N$	$8N$
$DST-I$	k_1+3	$k_1+k_2+k_3+5$		
$DST-II$	k_1+k_3+3	$k_1+k_2+k_3+3$		
$DST-III$	$2(N+1)^*+2$	$(4N+2log_2N+2)^*$		

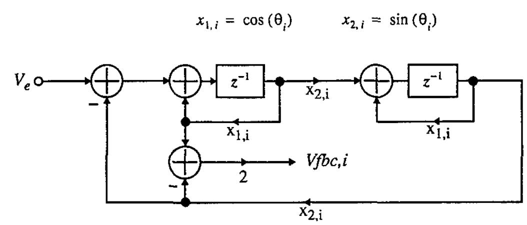

Fig. 4. Coupled-form biquad.

implement the $H_{fbc,i}(z)$). In Table V,

$$k_1 \triangleq 4\left[\lfloor\frac{N-1}{2}\rfloor + \lfloor\frac{N}{2}\rfloor\right] \approx 4N,$$

$$k_2 \triangleq \log_2\left[\lfloor\frac{N+3}{2}\rfloor\right] + \log_2\left[\lfloor\frac{N+4}{2}\rfloor\right] \approx 2\log_2\left[\frac{N}{2}\right],$$

and $k_3 \triangleq \lfloor\frac{N+1}{2}\rfloor + \lfloor\frac{N}{2}\rfloor \approx N.$

The signal flow graph of the filter-bank for the DCT-II, implemented using the S-V and V-S structures is shown in Fig. 5(a) and (b).[5]

IV. Finite Precision Effects

The modularity and linear complexity of the transformer structure make it very suitable for implementation using VLSI circuits or DSP's. As the internal wordlength and coefficient wordlength used in these cases is finite, the study of finite precision effects on this structure is of particular interest. Recall from Section 3.1.1 that the even and odd filter-banks take the form of first- or second-order resonators in a feedback loop, with the desired outputs being taken as linear combinations of the internal nodes of the filter structure. If the second-order resonators (with the transfer functions $H_{fbc,i}$) are implemented using the coupled-form biquad (see Fig. 4), then it can be shown that the poles of the filter-bank remain within the unit circle under coefficient quantization (assuming magnitude truncation), and that the filter structure is also free from limit cycles if magnitude truncation is used at the input of the delay elements. Under similar conditions, the poles of the frequency sampling structure also remain inside the unit circle; however, they lie very close to the unit circle, as shown by the example in Section 4.3. Also, the frequency sampling structure may sustain zero input limit cycles.

For the filter-bank, it is also possible to use other biquad structures such as LDI biquads, or direct-form biquads [18], [19]. Both these biquads have the advantage that even after coefficient truncation, the resonator poles lie on the unit circle (which is not the case for the coupled-form biquads), and their resonator frequencies are less sensitive to coefficient truncation as compared to the coupled-form, respectively, for resonator frequencies close to zero, and close to $\frac{f_s}{4}$. Even though the stability of the overall filter-bank under coefficient truncation is guaranteed with the use of these biquads, it has unfortunately not been possible to prove that the filter-bank will not sustain zero input limit cycles, though it is conjectured that this will be so. For this reason, we will only consider an implementation of the resonators using coupled-form biquads, for which we can prove both stability of the filter-bank under finite coefficient precision, and the absence of zero input limit cycles under finite internal wordlength. An additional advantage of using coupled-form biquads is that, if infinite precision coefficients are used, the internal states of the filter are exactly scaled in an L2 sense [18], [20]; even with finite precision coefficients, it is expected that the filter will remain well scaled.

[5] The * denotes complex operations. The coupled form is used to implement the second-order $H_{fbc,i}(z)$ and $H_{fb,i}(z)$, and a tree structure is used to add up all the $V_{fbc,i}$ in the feedback loop. Also, as the recursive formulas of [5] require both the DST and DCT to be maintained, and updated in order to compute a sliding transform, the numbers shown for [5], corresponding to the DCT-i in the table, refer to the computation required to obtain both the updated DCT-i and the DST-i values.

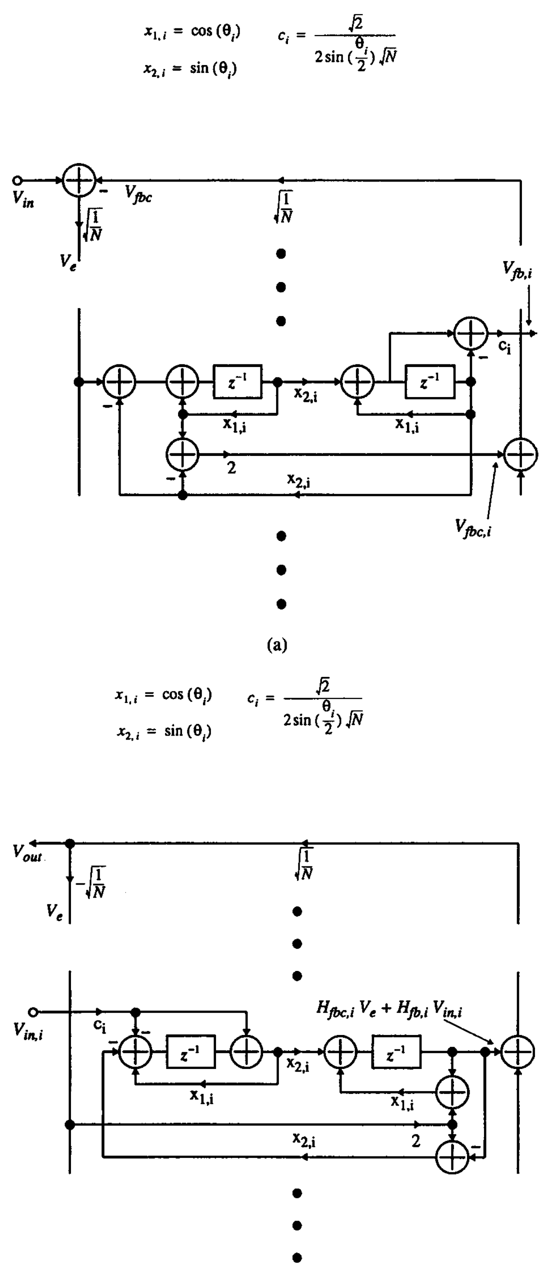

Fig. 5. (a) Implementation of either filter-bank of the S-V structure for DCT-II. (b)Implementation of either filter-bank of the V-S structure for DCT-II.

4.1. Stability

Let $x_{1,i} = \cos(\theta_i)$ and $x_{2,i} = \sin(\theta_i)$ represent the coefficients of the biquad in Fig. 4, implemented with infinite precision, and let $\hat{x}_{1,i} = Q[\cos(\theta_i)]$, $\hat{x}_{2,i} = Q[\sin(\theta_i)]$ represent the coefficients after magnitude truncation. The transfer function $H_{fbc,i} = V_{fbc,i}/V_e$ of Fig. 4 may now be derived to be

$$H_{fbc,i}(z) = -1 + H_{p,i}(z),$$
$$\text{where } H_{p,i}(z) = \frac{(1-(\hat{x}_{1,i}^2+\hat{x}_{2,i}^2)z^{-2})}{1-2\hat{x}_{1,i}z^{-1}+(\hat{x}_{1,i}^2+\hat{x}_{2,i}^2)z^{-2}}. \quad (20)$$

The poles of $H_{p,i}(z)$ are seen to be always complex, and, due to the coefficient truncation strategy (magnitude truncation), they also lie inside the unit circle, at a radius $\hat{r}_i = \sqrt{\cos^2(\hat{\theta}_{1,i})+\sin^2(\hat{\theta}_{2,i})} < 1$. Further, if the real part of $H_{p,i}(z)$ is evaluated on the unit circle, it may be shown to be always greater than zero (see Appendix A.2 for a proof of this, and the following statements in this section). Hence, the transfer function $H_{p,i}(z)$ may be related through the bilinear transform, $z \leftarrow (1+s)/(1-s)$, to a positive real s-domain transfer function [19], [21], [22]. Consequently, the real part of $H_{p,i}(z)$ can only take on positive values for z values outside, or on, the unit circle.

Now, consider the transfer function $H_e(z)$. Assuming that the coefficient $\sqrt{G}(= 1/\sqrt{N})$ of the filter-bank has been truncated to $\frac{\gamma}{\sqrt{N}}$, where $\gamma < 1$, it may be written as

$$H_e(z) = \frac{1}{g+\frac{\gamma^2}{N}\sum_i H_{p,i}(z)}, \text{ where } g = 1 - \frac{\gamma^2\lfloor\frac{N+1}{2}\rfloor}{N} > 0. \quad (21)$$

The poles of $H_e(z)$ occur at those values of z for which the sum of the real parts of $H_{p,i}(z)$ equals $-g$, and this cannot happen for values of z outside, or on the unit circle; hence, all the poles of $H_e(z)$ lie inside the unit circle.

4.2. Zero Input Limit Cycles

A sufficient condition for the absence of zero input limit cycles under magnitude truncation strategy was given in [23]. If $\underline{A}_{cl}, \underline{B}_{cl}, \underline{C}_{cl}$, and $\underline{D}_{cl}$ represent the state space description of the transfer function $H_e(z)$ of the filter-bank, *limit cycles are absent if* $\underline{I} - \underline{A}_{cl}^*\underline{A}_{cl}$ *is positive semi-definite.* As the filter-bank essentially embeds resonators in a feedback loop, we can express the closed loop state matrix $\underline{A}_{cl}$ in terms of the open loop state matrices $\underline{A}_{ol}, \underline{B}_{ol}, \underline{C}_{ol}$, and $\underline{D}_{ol}$ as $\underline{A}_{cl} = \underline{A}_{ol} - \underline{B}_{ol}\underline{C}_{col}$. For the filter-bank, $\underline{A}_{ol}$, $\underline{B}_{ol}$, and $\underline{C}_{ol}$ are given as follows : $\underline{A}_{ol}$ is block diagonal, with the i^{th} diagonal block being given by

$$\underline{A}_{ol,i} = \begin{bmatrix} \hat{x}_{1,i} & \hat{x}_{2,i} \\ -\hat{x}_{2,i} & \hat{x}_{1,i} \end{bmatrix} \quad (22)$$

$\underline{B}_{ol} = [(1/\sqrt{N})0(1/\sqrt{N})0\cdots]^T$, and $\underline{C}_{ol} = \underline{B}_{ol}^* A_{ol}$. We may now derive the following:

$$\underline{A}_{ol}^*\underline{A}_{ol} = \underline{I} - \underline{\epsilon},$$
$$\text{where } \underline{\epsilon} = \mathrm{diag}(1-\hat{r}_1^2, 1-\hat{r}_1^2, 1-\hat{r}_2^2, 1-\hat{r}_2^2, \ldots). \quad (23)$$

$$\underline{I} - \underline{A}_{cl}^*\underline{A}_{cl} = \underline{I} - \underline{A}_{ol}^*\underline{A}_{ol} + 2\left(1 - \sum_{i=0}^{l_2-1}\hat{r}_i^2\right)\underline{A}_{ol}^*\underline{B}_{ol}\underline{B}_{ol}^*\underline{A}_{ol}$$
$$= \underline{\epsilon} + 2\left(1 - \sum_{i=0}^{l_2-1}\hat{r}_i^2\right)\underline{A}_{ol}^*\underline{B}_{ol}\underline{B}_{ol}^*\underline{A}_{ol}, \quad (24)$$

where $\underline{\epsilon}$ is a positive definite diagonal matrix because $\hat{r}_i < 1$. Hence, the quantity $\underline{I} - \underline{A}_{cl}^*\underline{A}_{cl}$ in (24) is positive semi-definite. Consequently, zero input cycles may be eliminated in the filter-bank.[6]

4.3. FIR Behavior (Comparison with the Frequency Sampling Structure)

If infinite coefficient wordlength is used for either the generalized transformer, or the frequency-sampling structure, the impulse response of the transfer function from the input to $V_{fb,i}$ is FIR, with length equal to N. Under finite precision however, the poles of either structure move away from zero, and the impulse response becomes IIR. The poles of the generalized transformer however remain close to zero, while the poles of the frequency sampling structure remain close to the unit circle. This is illustrated in Fig. 6, where the error in the impulse response of the third channel of the "even" filter-bank is shown for the transformer structure and the frequency sampling structure corresponding to the DCT-II. (The error refers to the difference in the impulse response of the structure, implemented with infinite precision coefficients, and finite precision coefficients.) This simulation (carried out using double precision floating point arithmetic) uses a value of N equal to 32, and 9 bits (including one sign bit) to represent the internal coefficients. The error in the impulse response dies away to zero much more slowly for the case of the frequency-sampling structure, showing that its poles are closer to the unit circle.

V. Conclusion

A general filter-bank structure has been proposed, that is based on the NxN basis matrix of a transform, and can be used to implement "sliding" transforms of data. For the case of trigonometric transforms such as the DFT, DCT, and DST, it is similar to the frequency sampling structure; however, it is seen to have much better sensitivity properties, which arise because the structure involves the embedding of digital resonators, the "basis-generating" filters, in a feedback loop. It is also shown that certain earlier reported structures [6], [9] arise as special cases of this approach. This structure is also very hardware efficient for the case of trigonometric transforms; this along with its modularity, and good finite precision behavior make it a good candidate for VLSI implementation.

VI. Appendix

A.1. Necessity of a Minimal Implementation for the Generalized Transformer

Consider the $H_{fb,i}(z)$ for the DCT-II case, as given by (15). If the $H_{fb,i}(z)$ and $H_c(z)$ are implemented as a cascade of a

[6] As far as roundoff noise is concerned, the filter-bank structure is optimum [20], [24] if infinite coefficient precision is used. Hence, even with a slight degradation in noise performance, associated with the use of finite precision coefficients, it is conjectured that the structure will have good noise performance, and as the roundoff noise is an upper bound on the sensitivity [25], the structure should also have good sensitivity properties. These issues will be dealt with in more detail in [24].

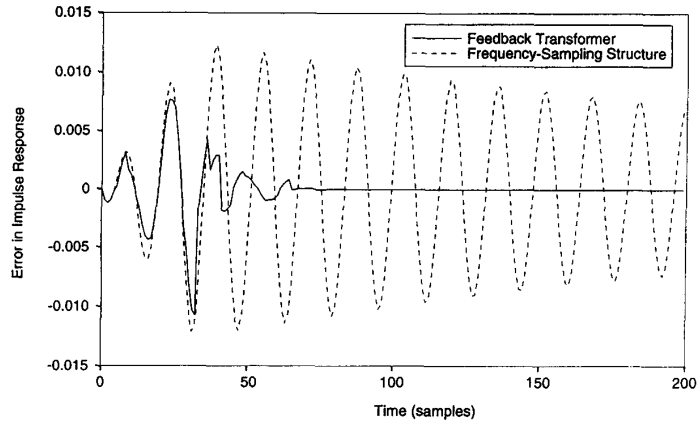

Fig. 6. Error in impulse response of generalized structure and frequency sampling structure.

Nth-order transfer function, $(z^{-N} + (-1)^i)/(1 + \eta z^{-K})$, and a second-order section,

$$+(z^{-1}(1 - z^{-1}))/(1 - 2\cos(\theta_i)z^{-1} + z^{-2})$$

then the transformer could be implemented using a single filter-bank as shown in Fig. 1, with a nonminimal number of delays in the feedback loop. The loop gain is now given by

$$\begin{aligned}\delta(z) &= G\sum_{i=0}^{N-1}\left(-\sqrt{\frac{2}{N}}k_i \frac{z^{-1}(1-z^{-1})\cos(\theta_i/2)}{1-2\cos(\theta_i)z^{-1}+z^{-2}}\frac{z^{-N}+(-1)^i}{1+\eta z^{-K}}\right)\\ &\quad + \frac{h_{c,1}z^{-1} + \cdots + h_{c,N-1}z^{-(N-1)}}{1+\eta z^{-K}}\\ &= \frac{a_1 z^{-1} + \cdots + a_{3N}z^{-3N}}{(1+\eta z^{-K})\prod_{i=0}^{N-1}(1 - 2\cos(\theta_i)z^{-1} + z^{-2})}\end{aligned} \tag{A.1}$$

where $a_1, \ldots, a_{3N}$ are some real numbers. The transfer function $H_e(z)$ now becomes

$$\begin{aligned}H_e(z) &= \frac{\sqrt{G}}{1+\delta(z)} = \\ &\frac{\sqrt{G}(1+\eta z^{-K})\prod_{i=0}^{N-1}(1-2\cos(\theta_i)z^{-1}+z^{-2})}{(1+\eta z^{-K})\prod_{i=0}^{N-1}(1-2\cos(\theta_i)z^{-1}+z^{-2})+a_1z^{-1}+\cdots+a_{3N}z^{-3N}}.\end{aligned} \tag{A.2}$$

Ideally, of course, $\delta(z) = \frac{-\eta z^{-K}}{1+\eta z^{-K}}$, and $\frac{1}{1+\delta(z)} = 1 + \eta z^{-K}$. This implies that all the terms $(1 - 2\cos(\theta_i)z^{-1} + z^{-2})$ in the numerator of (A.2), which represent zeros lying on the unit circle, cancel corresponding terms in the denominator. Hence, (A.2) has poles as well as zeros on the unit circle, which cancel exactly under infinite precision arithmetic, to produce a stable FIR transfer function. However, for finite precision, this cancellation will not occur, and the structure turns out to have poles very close to or on the unit circle. Hence, if the feedback loop is implemented with a nonminimal number of delays, the structure is as sensitive to coefficient truncation effects as the frequency sampling structure.

A.2. Stability of Finite Precision Implementation

We start with

$$H_{p,i}(z) = 1 - \hat{r}_i^2 z^{-2}/1 - 2\cos(\hat{\theta}_{1,i})z^{-1} + \hat{r}_i^2 z^{-2}$$

where $\hat{r}_i^2 = \cos^2(\hat{\theta}_{1,i}) + \cos^2(\hat{\theta}_{2,i}) < 1$. Evaluating this on the unit circle, we get

$$H_{p,i}(e^{j\omega}) = \frac{(1-\hat{r}_i^2)\cos(\omega) + j(1+\hat{r}_i^2)\sin(\omega)}{(1+\hat{r}_i^2)\cos(\omega) - 2\cos(\hat{\theta}_{1,i}) + j(1-\hat{r}_i^2)\sin(\omega)} \tag{A.3}$$

and taking the real part alone, we get

$$Re.\ H_{p,i}(e^{j\omega}) = \frac{1-\hat{r}_i^2}{|D|^2}\left[1 + \hat{r}_i^2 - 2\cos(\hat{\theta}_{1,i})\cos(\omega)\right] \tag{A.4}$$

where $|D|$ represents the magnitude of the denominator in (A.3). As the term $(1 - \hat{r}_i^2)/|D|^2$ is positive, the real part of $H_{p,i}(e^{j\omega})$ is lower bounded by

$$\begin{aligned}Re.\ H_{p,i}(e^{j\omega}) &> 1 + \cos^2(\hat{\theta}_{1,i})\\ &\quad + \sin^2(\hat{\theta}_{2,i}) - 2|\cos(\hat{\theta}_{1,i})| &\text{(A.5)}\\ &> (1 \pm \cos(\hat{\theta}_{1,i}))^2 + \sin^2(\hat{\theta}_{2,i}) &\text{(A.6)}\\ &> 0. &\text{(A.7)}\end{aligned}$$

Hence, the real part of $H_{p,i}(z)$ evaluated on the unit circle is strictly positive.

On positive-real functions and the bilinear transform: An s-domain transfer function, $H_a(s)$, is positive real if its real part is greater than zero everywhere in the right half of the s-plane [21]. Equivalent conditions for positive reality are

i) all poles of $H_a(s)$ lie in the left half plane:

ii) $Re.\ H_a(j\omega) \geq 0$; i.e., the real part of $H_a(s)$ evaluated on the j-axis is greater than or equal to zero.

Now, the bilinear transform, $s \leftarrow z - 1/z + 1$, maps the j-axis, the left half plane, and the right half plane of the s-domain, respectively, to the unit circle, inside the unit circle, and outside the unit circle in the z-domain. Consequently, applying the bilinear transform on a positive real $H_a(s)$, results in $H_d(z)$, whose real part is greater than or equal to zero on, and outside the unit circle. Equivalent conditions that guarantee positive reality of $H_d(z)$ may be obtained simply by transforming the equivalent conditions in the s-domain to the z-domain through the bilinear transform; i.e., i) $H_d(z)$ has its poles inside the unit circle, and ii) its real part evaluated on the unit circle is always greater than zero.

ACKNOWLEDGMENT

We would like to thank Dr. Farden and the reviewers for their detailed perusal of the manuscript, and Prof. Peceli for drawing our attention to [4].

REFERENCES

[1] S. S. Narayan, A. M. Peterson, and M. J. Narasimha, "Transform domain LMS algorithm," *IEEE Trans. on Acoust. Speech, Signal Processing*, vol. 31, pp. 609–615, June 1983.
[2] D. F. Marshall, W. K. Jenkins, and J. J. Murphy, "The use of orthogonal ransforms for improving performance of adaptive filters," *IEEE Trans. Circuits Syst.*, vol. 36, pp. 474–483, Apr. 1989.
[3] N. Ahmed and K. R. Rao, *Orthogonal Transforms for Digital Signal Processing*. New York: Springer-Verlag, 1975.
[4] J. A. Stuller, "Generalized running discrete transforms," *IEEE Trans. Acoust., Speech, Signal Processing*, vol. 30, pp. 60–68, Feb. 1982.
[5] P. Yip and K. R. Rao, "On the shift property of DCT's and DST's," *IEEE Trans. Acoust., Speech, Signal Processing*, vol. 35, pp. 404–406, Mar. 1987.
[6] G. Peceli, "A common structure for recursive discrete transforms," *IEEE Trans. Circuits Syst.*, vol. 33, pp. 1035–1036, Oct. 1986.
[7] A. V. Oppenheim and R. W. Schafer, *Digital Signal Processing*. Englewood Cliffs, NJ: Prentice-Hall, 1975.
[8] G. H. Hostetter, "Recursive discrete Fourier transformation," *IEEE Trans. Acoust., Speech, Signal Processing*, vol. 28, pp. 184–190, Apr. 1980.
[9] G. Peceli and B. Feher, "Digital filters based on recursive Walsh-Hadmard transformation," *IEEE Trans. Circuits Syst.*, vol. 37, pp. 150–152, Jan. 1990.
[10] C. L. Gundel, "Filter Bank Interpretation of DFT and DCT," in *EURASIP*, pp. 643–646, 1988.
[11] M. Vetterli, "Tree structures for orthogonal transforms and applications to the Hadamard transform," *Signal Processing*, vol. 5, pp. 473–484, Nov. 1983.
[12] R. R. Bitmead, "On recursive discrete Fourier transformation," *IEEE Trans. Acoust., Speech, Signal Processing*, vol. 30, pp. 319–322, Apr. 1982.
[13] G. Peceli, Private communication, 1992.
[14] H. S. Hou, "A fast Recursive algorithm for computing the discrete cosine transform," *IEEE Trans. Acoust. Speech, Signal Processing*, vol. 35, pp. 1455–1461, Oct. 1987.
[15] K. R. Rao and P. Yip, *Discrete Cosine Transform*. New York: Academic Press, 1990.
[16] C. Loeffler, A. Ligtenberg, and G. S. Moschytz, "Practical fast 1-D DCT algorithms with 11 multiplications," in *Proc. Int. Conf. Acoustics, Speech, and Signal Processing*, pp. 988–991, May 1989.
[17] R. R. Bitmead and B. D. O. Anderson, "Adaptive frequency sampling filters," *IEEE Trans. Circuits Syst.*, vol. 28, pp. 524–534, June 1981.
[18] M. Padmanabhan, "Feedback-based orthogonal digital filters, their application in signal processing, and their VLSI Implementation," Ph.D. dissertation, Univ. California, Los Angeles, 1992.
[19] M. Padmanabhan and K. Martin, "Resonator-based filter-banks for frequency-domain applications," *IEEE Trans. Circuits Syst.*, vol. 38, pp. 1145–1159, Oct. 1991.
[20] G. Peceli, "Resonator-based digital filters," *IEEE Trans. Circuits Syst.*, vol. 36, pp. 156–159, Jan. 1989.
[21] G. C. Temes and J. W. LaPatra, *Introduction to Circuit Synthesis and Design*. New York: McGraw-Hill, 1977.
[22] W. F. McGee and G. Zhang, "Logarithmic filter banks," in *Proc. Int. Symp. Circuits and Systems*, pp. 661–664, 1990.
[23] P. P. Vaidyanathan and V. Liu, "An improved sufficient condition for absence of limit cycles in digital filters," *IEEE Trans. Circuits Syst.*, vol. 34, pp. 319–322, Mar. 1987.
[24] M. Padmanabhan and K. Martin, "Feedback-based orthogonal digital filters," *IEEE Trans. Circuits Syst.*, to be published, 1993.
[25] L. B. Jackson, "Roundoff noise bounds derived from coefficient sensitivities for digital filters," *IEEE Trans. Circuits Syst.*, vol. 23, pp. 481–485, Aug. 1976.

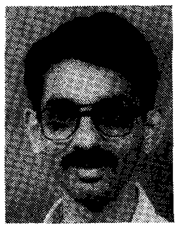

Mukund Padmanhaban received the B. Tech. (Honors) degree from the Indian Institute of Technology, Kharagpur, in 1987, and the M.S. and Ph.D. degrees in electrical engineering from the University of California, Los Angeles, in 1989 and 1992, respectively.

He is currently with the Speech Recognition Group at the IBM T.J. Watson Research Center, Hawthorne, NY. His research interests are in signal processing, digital and analog filters, speech processing, and analog integrated circuits.

Ken Martin (S'75–M'80-SM'89-F'91) received the B.A.Sc. (graduating at the top of his class) and the M.A. Sc. from the University of Toronto in 1975 and 1977, repectively, and the Ph.D. in 1980.

From 1977 to 1978, he was a member of the Scientific Research Staff at Bell Northern Research, Ottawa, Canada, where he did some of the early research in integrated switched-capacitor networks. Between 1980 and 1992, he was consecutively an assistant, an associate, and a full professor at the University of California, Los Angeles. In 1992, he accepted the Stanley Ho Professorship in Microelectronic at the University of Toronto. He has been a consultant to many companies, including Xerox, Hughes Aircraft, Intel, and Brooktree, in the areas of high-speed analog and digital integrated circuit design. He has ongoing research programs in the areas of analog CMOS and BiCMOS systems, high-speed GaAs MESFET and HBT circuits, and digital signal processing algorithms for fixed and adaptive filters. He was appointed as the Circuits and Systems IEEE Press Representative in 1985. He was selected by the Circuits and Systems Society for the Outstanding Young Engineer Award that was presented at the IEEE Centennial Keys to the Future Program in 1984. He was elected by the Circuits and Systems Society members to their administrative committee (1985–1987). He served as an associate editor of the IEEE TRANSACTIONS ON CIRCUITS AND SYSTEMS from 1985 to 1987, and has served on the technical committee for many international symposia on circuits and systems. He is currently an Associate Editor for the IEEE Proceedings.

Professor Martin was awarded a National Science Foundation Presidential Young Investigator Award that ran from 1985 to 1990.